

System Identification for Limit Cycling Systems: A Case Study for Combustion Instabilities*

R. M. Murray[†] C. A. Jacobson[‡] R. Casas[§] A.I Khibnik[¶] C.R. Johnson Jr.^{||}
R. Bitmead^{**} A.A. Peracchio^{††} W.M. Proscia^{‡‡}

September 15, 1997

Abstract

This paper presents a case study in system identification for limit cycling systems. The focus of the paper is on (a) the use of a model structure derived from physical considerations and (b) the use of algorithms for the identification of component subsystems of this model structure. The physical process used in this case study is that of a reduced order model for combustion instabilities for lean premixed systems. The identification techniques applied in this paper are the use of linear system identification tools (prediction error methods), time delay estimation (based on Kalman filter harmonic estimation methods) and qualitative validation of model properties using harmonic balance and describing function methods. The novelty of the paper, apart from its practical application, is that closed loop limit cycle data is used together with a priori process structural knowledge to identify both linear dynamic forward and nonlinear feedback paths. Future work will address the refinement of the process presented in this paper, the use of alternative algorithms and also the use of control approaches for the validated model structure obtained from this paper.

Contents

1 Introduction

2

*This paper has been submitted for publication in the proceedings of the 1998 American Control Conference. It has been supported in part by United Technologies Research Center, DARPA Contract MDA 972-95-C-009 and NSF Grant ECS-9528363.

[†]California Institute of Technology, Mail Code 104-44, Pasadena, CA 91125, 626 395-6460, murray@indra.caltech.edu

[‡]United Technologies Research Center, MS15, 411 Silver Lane, East Hartford, CT 06108, 860 610 7652, jacobsc@utrc.utc.com

[§]School of Electrical Engineering, Frank H.T. Rhodes Hall, Cornell University, Ithaca, NY 14853, 607 254 8819, raulc@anise.ee.cornell.edu

[¶]United Technologies Research Center, MS15, 411 Silver Lane, East Hartford, CT 06108, 860 610 7403, khibniai@utrc.utc.com

^{||}School of Electrical Engineering, Frank H.T. Rhodes Hall, Cornell University, Ithaca, NY 14853, 607 255 9042, johnson@anise.ee.cornell.edu

^{**}Cooperative Research Centre for Robust and Adaptive Systems, Institute of Advanced Studies, Australian National University, Canberra, ACT 0200, Australia 02 6279 8612, bob@syseng.anu.edu.au

^{††}United Technologies Research Center, MS19, 411 Silver Lane, East Hartford, CT 06108, 860 610 7815, peraccaa@utrc.utc.com

^{‡‡}United Technologies Research Center, MS30, 411 Silver Lane, East Hartford, CT 06108, 860 610 7679, prosciw@utrc.utc.com

2	Model Description	3
2.1	Acoustic model	3
2.2	Heat Release Model	4
2.3	Summary of the equations	6
3	Analytical Stability Analysis of Combustion Model	6
3.1	Stability criteria	7
3.2	Nonlinear stability analysis	9
3.3	Globalization	10
4	System Identification Methodology: A Case Study	12
4.1	Linear System Identification	14
4.2	Time Delay Identification	14
4.2.1	Bulk Delay Estimation	16
4.2.2	Time-Varying Delay Estimation	16
4.3	Parameterization of Static Nonlinearity	17
4.4	Validation by Harmonic Balance	19
5	Concluding Remarks	23
6	Acknowledgments	23

1 Introduction

The objective of this effort is to obtain a system identification methodology for dynamical systems that exhibit limit cycle behavior. Nonlinear dynamical systems that exhibit self excited oscillations are common both in terms of constraints imposed by control mechanisms, such as saturation, but also in physical processes themselves. The system identification problem considered in this paper is to consider the limit cycle behavior as a qualitative constraint on the identification methodology. That is, the system identification procedure must yield a match to the data so that the identified model exhibits a stable self excited oscillation.

The class of systems under consideration that exhibit self excited oscillations must necessarily be nonlinear. In essence, this implies that a considerable amount of physical insight is required to obtain a model structure capable of displaying the correct qualitative behavior. The general description of methods considered for system identification of limit cycling systems will be reduced to a parameter estimation problem (in finite dimensions) that arises from the physical description of the process. The partition of the methods thus reduces naturally to (a) studying the behavior of standard parameter estimation schemes on problems of interest and (b) developing special algorithms that constrain the identification of limit cycling systems.

This paper concentrates on presenting a physical problem of some technological interest and studying the behavior of standard estimation procedures on experimental data in an effort to obtain qualitatively correct models, that is, models that display stable limit cycle behavior in the final selection of parameters. The context of this study into the use of existing system identification tools is the identification of dynamics of a combustion instability process. The example is taken from a technologically relevant area of lean premixed combustion processes where the dynamics appear to be governed by self excited oscillations of the amplitude of which is governed by the combustor fuel-air ratio. The ultimate goal of studying system identification in the context of this system is

to be able to apply adaptive regulation with confidence to these types of dynamics, hence, the open loop study presented in this paper is but a necessary first step in an overall research plan.

The organization of the paper is as follows. The combustion dynamics model used as an example is presented in Section 2 and brief comments regarding the qualitative dynamics are given. Section 4 presents the identification methodology for this case study. Section 5 gives conclusions and comments on future directions for this kind of investigation.

2 Model Description

This paper uses a reduced order model for the combustion system. The purpose of this section is to describe briefly the reduced order model that includes a nonlinear heat release model under development [17] for lean premixed combustion systems.

A brief review of related work (and citations to other work) is as follows. The study of combustion instabilities similar to the system studied in the current paper can be found in [3, 14, 24]. System models of combustion that are relevant to this paper, especially some that contain models that exhibit limit cycle dynamics can be found in [7, 4, 5, 17, 12]. The work of [17] is followed below and is briefly described in this section to give some understanding of the model structure used for identification. The model consists of acoustic and heat release subsections and are described in 2.1 and 2.2 below.

2.1 Acoustic model

The equations of motion for an inviscid, non-conducting fluid can be written as

$$\frac{\partial \rho}{\partial t} + \nabla \cdot (u\rho) = 0 \quad (1)$$

$$\rho \frac{\partial u}{\partial t} + \rho u \cdot \nabla u = -\nabla p \quad (2)$$

$$\frac{\partial p}{\partial t} + \gamma p \nabla \cdot u + u \cdot \nabla p = (\gamma - 1)q, \quad (3)$$

where ρ , p , and u are the density, pressure, and velocity fields, and q is the rate of heat addition. Equations (1) and (2) are the Navier-Stokes equations and equation (3) is derived from energy considerations. The fluid is assumed to be a perfect gas with constant specific heat. The constant γ is the ratio of specific heats.

One can now expand the flow fields into mean and fluctuating components:

$$u = \bar{u} + u' \quad p = \bar{p} + p' \quad q = \bar{q} + q'.$$

By taking the time derivative of equation (1) and using the momentum equation (2), the (linearized) wave equation with forcing is

$$\frac{\partial^2 p'}{\partial t^2} - a^2 \nabla^2 p' = (\gamma - 1) \frac{\partial q'}{\partial t}, \quad (4)$$

where a is the (average) speed of sound. The boundary condition for the wave equation is given by

$$n \cdot \nabla p' = -f,$$

where n is the outward normal vector on the boundaries of the chamber and f is the projection of the (fluctuating) momentum equation onto the normal direction.

A solution for these equations can be obtained by expanding the solution in terms of the orthogonal acoustic modes of the system, Ψ_i , defined by the eigenvalue problem

$$\nabla^2 \Psi_i + k_i^2 \Psi_i = 0 \quad (5)$$

$$n \cdot \nabla \Psi_i = 0 \quad (6)$$

where ω_i is the frequency of the i th mode and $k_i = \omega_i/a$ is the wavenumber for the i th mode. The solution is expanded in terms of these modes:

$$p' = \bar{p} \sum \eta_i(t) \Psi_i(x).$$

This yields, for longitudinal acoustic modes,

$$\ddot{\eta}_i + 2\alpha\dot{\eta}_i + \omega_i^2 \eta_i = \frac{\gamma - 1}{\bar{p}E_i^2} \int \Psi_i(x) \frac{\partial q'}{\partial t}(x, t) dx \quad (7)$$

where

$$E_i^2 = \int \Psi_i^2(x) dx$$

is a normalizing factor. Note that in this formulation, the *rate* of the heat release rate drives the equations. It is important to remember that equation (7) only describes the amplitude of the *fluctuations*; q' is defined as the fluctuations about the mean.

2.2 Heat Release Model

In order to model the heat release, an “actuator disk” model is assumed in which all heat is released into the fluid at a point, denoted x_f . This reduces equation (7) to the form

$$\ddot{\eta}_i + \omega_i^2 \eta_i = \frac{\gamma - 1}{\bar{p}E_i^2} \Psi_i(x_f) \frac{\partial}{\partial t} q'_A(t) =: N \frac{\partial}{\partial t} q'_A(t)$$

where $q'_A(t)$ is the heat release rate per unit cross-sectional area [W/m²].

Following [17] the heat release rate is written as

$$q_A(t) = \bar{q}_A + q'_A = \frac{\rho_m S_u A_f(t) \Delta H_m(t)}{A_c} \quad (8)$$

where

ρ_m	= density of fuel/air mixture (constant)	[kg/m ³]
S_u	= flame speed	[m/s]
A_f	= instantaneous flame surface area	[m ²]
A_c	= combustor cross-sectional area	[m ²]

and $\Delta H_m(t)$ is the heat of combustion of the mixture reaching the flame front at time t .

Assuming that the fuel mixture convects from the injection nozzle to the flame front, the heat of combustion can be written as a function of the inlet equivalence ratio τ_v seconds earlier,

$$\Delta H_m(t) = \Delta H_m(\phi(t - \tau_v)|_{x=0}),$$

where τ_v is the convective time delay and ϕ is the equivalence ratio. Letting W_F represent the fuel mass flow and W_A the air mass flow,

$$\phi = \frac{W_F/W_A}{(W_F/W_A)_s},$$

where the denominator is the stoichiometric ratio. The convective time lag can be approximately computed from the mean flow speed and the flame location x_f , but should also be modified to include nozzle mixing times.

Remark 2.1 *This model assumes that all mixing between the air and fuel occurs at the nozzle and hence the air velocity in the nozzle determines the equivalence ratio at time $t - \tau$. This perfectly mixed gas then transports down the combustion chamber and reaches the burning plane τ seconds later. If substantial mixing occurs across a distributed area, a more accurate model of this might be required.*

At this point it remains to specify the dependence of the heat of combustion on the equivalence ratio, the dependence of the equivalence ratio on the pressure oscillations in the system, and the dependence of the flame area on pressure fluctuations.

Dependence of heat of combustion on equivalence ratio The dependence of the heat release per unit mass of mixture on the equivalence ratio is approximately linear up to stoichiometric. After stoichiometric, we assume that the heat of combustion falls off roughly exponentially. An approximate model is given by

$$\frac{\Delta H_m}{\Delta H_s} = \begin{cases} 0 & \phi \leq 0 \\ N_s \left(1 - \frac{(\phi/k)^p}{1 + (\phi/k)^p} \right) \phi & 0 < \phi \leq 1 \\ \phi e^{(1-\phi)} & \phi > 1 \end{cases}$$

where ΔH_s is the heat of combustion for the stoichiometric mixture and N_s, k, p are constants for the specific fuel used.

Remark 2.2 *Discussions in [17] indicate that there might be situations where the heat of combustion does not fall off after stoichiometric and instead saturates. Also, there is an LBO (lean blow out) like limit at some $\phi > 0$ (instead of at the origin).*

Equivalence ratio variations The equivalence ratio is given by

$$\phi = \frac{W_F/W_A}{(W_F/W_A)_s},$$

The assumption is that the fuel flow is constant and that the instantaneous air flow depends on the velocity fluctuations generated by the longitudinal waves. Thus in the fuel preparation zone (nozzle)

$$\frac{\phi}{\bar{\phi}} = \frac{\bar{W}_A}{W_A} = \frac{\rho_m A_c \bar{u}}{\rho_m A_c (\bar{u} + u')} = \frac{1}{1 + u'/\bar{u}}$$

and hence

$$\phi(t - \tau_v) = \frac{\bar{\phi}}{1 + \tilde{u}(t - \tau_v)} \tag{9}$$

where $\tilde{u} = u'/\bar{u}$.

Combining the maps $\tilde{u} \mapsto \phi$ and $\phi \mapsto \Delta H_m$, we obtain the nonlinear map between local velocity at the inlet and the heat release.

Flame area propagation Roughly speaking, the flame surface area can be described as a function of the flow speed at the burning plane [6]. A first order lag is used to model the dynamics of the flame, and hence

$$\frac{d\tilde{A}_F}{dt} = b_1(\tilde{u} - \tilde{A}_F)$$

where

$$b_1 = \frac{G_o S_u}{R}$$

is the flame surface response time and

$$\begin{aligned} S_u &= \text{flame speed} & [\text{m/s}] \\ R &= \text{combustor radius} & [\text{m}] \\ G_o &= \tilde{A}_F = A'_F / \bar{A}_F \end{aligned}$$

2.3 Summary of the equations

Combining the computations above for a single acoustic mode a set of ordinary differential equations that describe the evolution of the system is obtained. At this point one additional assumption is made, namely, the velocity of the flow field to be proportional to the derivative of pressure. More precisely it is assumed that $u = \dot{\eta}$, which is true for the homogeneous (unforced) dynamics in the chamber.

Using this assumption, we can write the dynamics as

$$\ddot{\eta} + 2\alpha\dot{\eta} + \omega_i^2\eta = N \frac{d}{dt} \left((1 + \tilde{A}_F) \Delta H_m(\dot{\eta}(t - \tau), \bar{\phi}) \right) \quad (10)$$

$$\dot{\tilde{A}}_F = b_1(\sigma\dot{\eta} - \tilde{A}_F) \quad (11)$$

where \tilde{A}_F is the normalized flame area perturbation. This model structure (excluding the flame area equation) is shown in Figure 1.

3 Analytical Stability Analysis of Combustion Model

The purpose of this section is to carry out the stability and bifurcation analysis of the model derived in the previous section. Note that this model falls into a category of neutral differential equations [10]. We rewrite the model — for one mode and with obvious changes in notation — in the following form

$$\ddot{\eta} + 2\alpha\dot{\eta} + \omega^2\eta = N \frac{d}{dt} [H(\dot{\eta}(t - \tau)) (1 + A)], \quad (12)$$

$$\dot{A} = b_1(\sigma\dot{\eta} - A). \quad (13)$$

We assume that nonlinearity $H(\cdot)$ as well as some other model coefficients implicitly depend on $\bar{\phi}$, and that $H(\cdot)$ monotonically decreases saturating both at the left and at the right. The parameter values of interest satisfy conditions $\alpha/\omega \ll 1$, $1/\omega \ll 1$ and $b_1/\omega \ll 1$ which allows the use of averaging techniques for computing limit cycles and analyzing the associated stability. For $N = 0$ equation (12) decouples from equation (13) and turns into a weakly damped linear pendulum

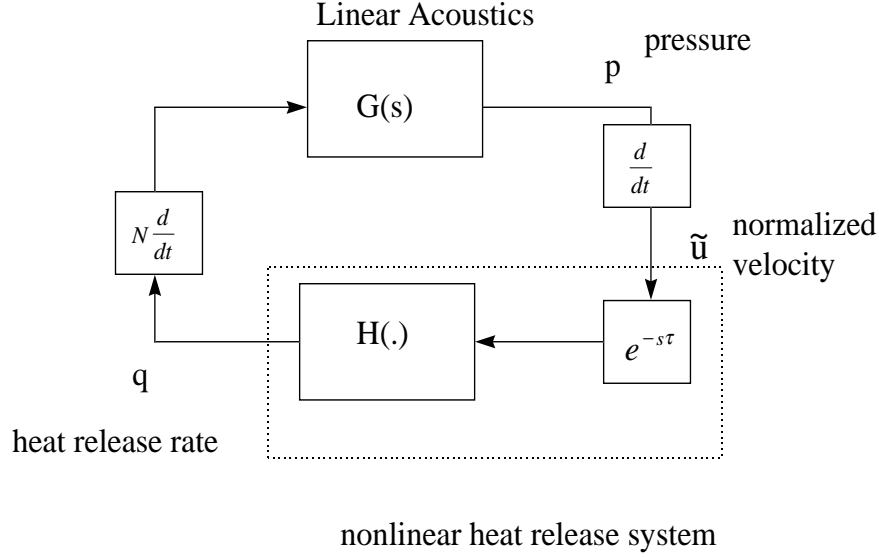


Figure 1: Block Diagram Structure of Combustion Model

equation. For a weak nonlinearity, equations (12) and (13) become coupled, but the zero solution remains stable. Weak nonlinearity means $N \ll 1$ and for $\eta = \cos(\omega t)$ and after appropriate scaling the nonlinearity is of the order NH' (H' is bounded). The destabilizing effect of the nonlinearity may overcome the stabilizing effect of damping if $N|H'(0)| > 2\alpha/\omega$; this is a rough estimate which will be detailed further. If instability occurs this should normally lead to an oscillatory type behavior, a limit cycle in the simplest case. Furthermore, under the condition $2\alpha/\omega < N|H'(0)| \ll 1$ we can expect the limit cycle to be approximated by an invariant curve of the unperturbed equation, the ellipse $\omega^2\eta^2 + \dot{\eta}^2 = R^2$. The unlimited growth of the amplitude of oscillations is impossible due to the damping effect of nonlinearity for large amplitudes: in this case both H and H' are relatively small for the large portion of the cycle which allows linear damping to suppress large-amplitude oscillations. For the purposes of bifurcation analysis it is assumed that coefficients N and τ are varied and coefficients α, ω, b_1 and σ are fixed.

3.1 Stability criteria

Linearizing (12),(13) about the origin $(\eta, \dot{\eta}, A) = (0, 0, 0)$ yields

$$\ddot{\eta} = -\omega^2\eta - 2\alpha\dot{\eta} + N \left[h_1\ddot{\eta}(t - \tau) + h_0\dot{A} \right], \quad (14)$$

$$\dot{A} = b_1(\sigma\dot{\eta} - A). \quad (15)$$

where $h_0 = H(0)$, $h_1 = H'(0)$. Substituting the harmonic solution $\eta = \sin \Omega t$, $A = (C_1 \sin \Omega t + C_2 \cos \Omega t)$ into (3.1), yields two constraints which define the parameters for the onset of Hopf bifurcation:

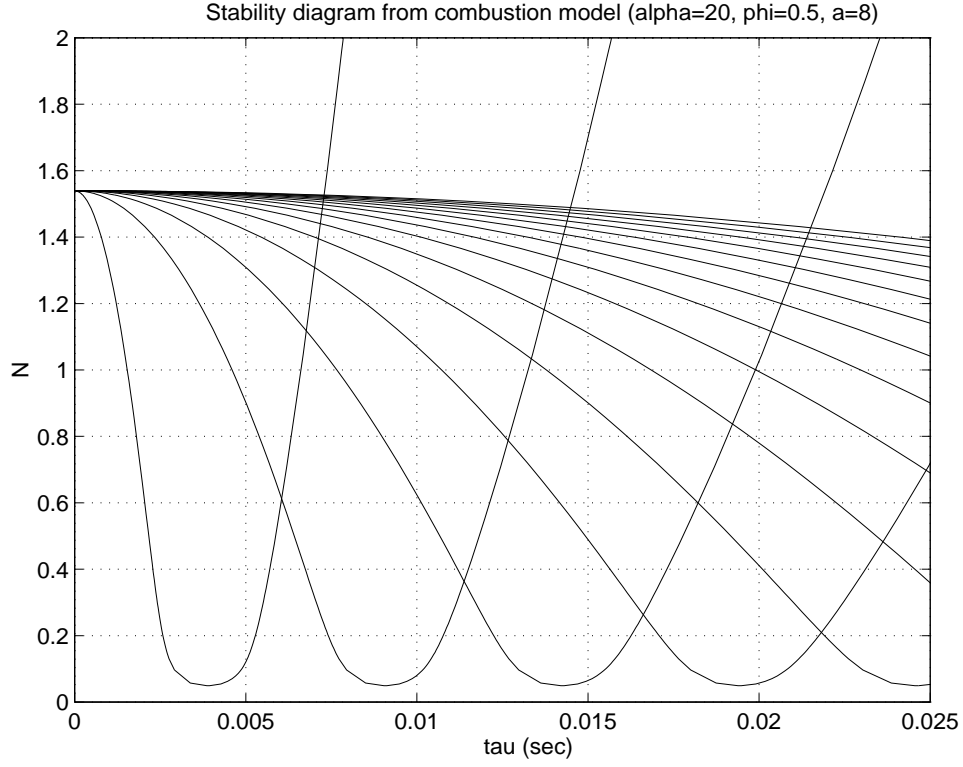


Figure 2: Stability Diagram for Reduced Order Combustion Model

$$-2\alpha + Nh_1\Omega \sin \theta + Nb_1\sigma h_0 \frac{\Omega^2}{\Omega^2 + b_1^2} = 0 \quad (16)$$

$$\omega^2 - \Omega^2 + Nh_1\Omega^2 \cos \theta + Nb_1^2\sigma h_0 \frac{\Omega^2}{\Omega^2 + b_1^2} = 0 \quad (17)$$

where $\theta = \Omega\tau$. Because the last term in (16) and (17) are small compared to the remaining term it is possible to solve approximately for N and τ :

$$\begin{aligned} \tau &= \arctan \frac{2\alpha\Omega}{\Omega^2 - \omega^2} + \pi k, k\text{--integer} \\ N &= \text{sign}(\sin(\theta)) \frac{\sqrt{4\alpha^2\Omega^2 + (\omega^2 - \Omega^2)^2}}{h_1\Omega^2} \end{aligned} \quad (18)$$

Recall that $h_1 < 0$ so that, for positive N , θ should be taken in the interval $\pi < \theta < 2\pi \pmod{2\pi}$. The graph of $N(\Omega)$ has a parabolic shape with minimum at $\Omega = \omega$. Note that if $\alpha \ll \omega$, then at the minimum $\theta \approx 3\pi/2$ and $N \approx |2\alpha/(h_1\Omega)|$. The same form of the graph holds also for system (16),(17). Increasing N and crossing the stability boundary changes the equilibrium point from stable to unstable.

Returning to the original delay parameter τ , $\tau = \theta/\Omega$, a more complicated structure of the stability boundary as shown in Figure 2 is obtained. Although single-frequency oscillations are the most typical outcome of crossing the stability boundary, the repetition of the same pattern due to

the adding of a multiple of the period to θ , combined with scaling by $1/\Omega$, leads to the interaction between different branches of the stability boundary. At each intersection point, called double Hopf point, two modes of instability, with different frequencies, occur simultaneously. Crossing the stability boundary through such a point, say as N increases, will in general have two possible scenarios: (1) two stable limit cycles arise simultaneously or (2) stable invariant two-dimensional torus arises, with two-frequency quasiperiodic motion on it (see [9] for a general reference and [19] for the particular case of neutral equations).

3.2 Nonlinear stability analysis

The purpose of this section is to present techniques for computing criticality conditions on the stability boundary. These conditions are usually expressed in terms of first Lyapunov quantity L_1 [9]. For L_1 negative, crossing the stability boundary from a stable to an unstable region gives rise to a stable limit cycle around the unstable equilibrium point. For L_1 positive, crossing the stability boundary from unstable to stable region gives birth to an unstable limit cycle surrounding the stable equilibrium point. Computing L_1 in “standard” delay equations is discussed in [11]; we are not aware of any extension of these techniques to neutral delay equations. For this latter case, we apply here the set of ideas close to averaging and harmonic balance (see [20] and [15]). Namely, the problem is posed of finding the limit cycles of small amplitude r and period $2\pi/\Omega$ assuming it is close to the circle

$$\eta^2 + (\eta')^2 = r^2 \quad (19)$$

where prime ($'$) denotes differentiation with respect to $\varphi = \Omega t$. To simplify exposition, we will assume from now that $A \equiv 0$. That is, we consider only (12), rewritten using φ and θ , as:

$$\eta'' + \frac{\omega^2}{\Omega^2}\eta = -\frac{2\alpha}{\Omega}\eta' + \frac{N}{\Omega} \frac{d}{d\varphi} [H(\Omega\eta'(\varphi - \theta))] \quad (20)$$

Note that, because of the assumption $2\alpha/\Omega \ll 1$ and $N \ll 1$, (20) can be seen as a perturbed pendulum equation.

Let the Taylor expansion of $H(u)$ at zero be $H(u) = h_0 + h_1u + \frac{h_2}{2}u^2 + \frac{h_3}{6}u^3 + \dots$. Differentiating (19) and using (20), with $\eta = r \sin \varphi$, the following equation for r is obtained:

$$r' = \frac{2\alpha r}{\Omega} \left[\frac{\Omega^2 - \omega^2}{2\alpha\Omega} \sin \varphi - \cos \varphi - \frac{N\Omega}{2\alpha} H'(\Omega r \cos(\varphi - \theta)) \sin(\varphi - \theta) \right] \cos \varphi \quad (21)$$

Now exploit the assumption that $2\alpha/\Omega$ is a small parameter to average (21) with respect to φ and obtain the average equation governing the amplitude only. Before doing that, replace $H(u)$ by its Taylor expansion and truncate terms of the order higher than three:

$$r' = \frac{2\alpha r}{\Omega} [g_1(\varphi) + g_2(\varphi)r + g_3(\varphi)r^2] \cos \varphi \quad (22)$$

where

$$\begin{aligned} g_1(\varphi) &= \frac{\Omega^2 - \omega^2}{2\alpha\Omega} \sin \varphi - \cos \varphi - h_1 \frac{N\Omega}{2\alpha} \sin(\varphi - \theta) \\ g_2(\varphi) &= -h_2 \frac{N\Omega^2}{2\alpha} \sin(\varphi - \theta) \cos(\varphi - \theta) \\ g_3(\varphi) &= -h_3 \frac{N\Omega^3}{4\alpha} \sin(\varphi - \theta) \cos^2(\varphi - \theta) \end{aligned} \quad (23)$$

Integrating (22) over interval $\varphi \in [0, 2\pi]$ the slow averaged equation for r is obtained:

$$\frac{dr}{ds} = \lambda r + Lr^3 \quad (24)$$

where

$$\begin{aligned} \lambda &= -1 + h_1 \frac{N\Omega}{2\alpha} \sin \theta \\ L &= h_3 \frac{N\Omega^3}{16\alpha} \sin \theta \end{aligned} \quad (25)$$

and $s = (2\alpha/\pi\Omega)\varphi$ is a slow time. Since on the stability boundary $\sin \theta < 0$, the sign of L is found to be opposite to the sign of h_3 .

In the averaged equation (24) λ determines the linear decay rate for the amplitude. When λ is zero or small the value of L becomes crucially important: For $L < 0$ (i.e. $h_3 > 0$) - so called supercritical case - the amplitude decays even for λ positive, given that the initial amplitude isn't "too small." For $\lambda > 0$ it will eventually approach stable fixed point $r^* = (-\lambda/L)^{1/2}$ which corresponds to a stable limit cycle in the original equations. In the opposite, called subcritical, case $L > 0$ (i.e. $h_3 < 0$) the amplitude grows even for λ negative assuming as before that the initial amplitude isn't "too small." Here for $\lambda < 0$ there exist an unstable fixed point $r^* = (-\lambda/L)^{1/2}$ which can be associated with unstable limit cycle. Note that "too small" means here initial amplitudes smaller than r^* . Both these scenarios can be realized in the combustion model.

3.3 Globalization

The globalization of the averaging procedure described above is an attempt to obtain and use the equation for the dynamics of the limit cycle amplitude like that in (24) to predict the amplitude and the stability of limit cycles not only for parameters close to the stability boundary but for also for parameters "far away" from that boundary. Formally averaging (21) and integrating by parts yields:

$$\frac{dr}{ds} = -r + \frac{N}{2\alpha\pi} \int_0^{2\pi} H(\Omega r \cos(\varphi - \theta)) \sin \varphi d\varphi \quad (26)$$

The hope is that (26) will approximate the actual dynamics of the amplitude of oscillations and particularly give a good approximation for the limit cycle amplitude. Note that, if the assumption of parameters being close to the stability boundary is violated then the frequency Ω in (20) and therefore in its averaged version (26) is formally unknown and should be chosen. The natural choice for Ω would be the frequency of the linear system for the corresponding values of parameters. By checking that this (linear based) frequency does not change much as we change model parameters, say N , it is possible to simplify things even further by assuming that Ω is the Hopf frequency corresponding to crossing the stability boundary. That is it is the *resonant* frequency computed from (18).

It should be emphasized that, under more general conditions, particularly when the unperturbed system is nonlinear, we will not be able to use the same frequency for perturbing different closed orbits and for different parameter values, particularly not lying close to the stability boundary. For nonlinear conservative systems the frequency is normally a nonconstant function of the amplitude and may vary substantially, even in some cases tending to zero (e.g. for conservative system

Amplitude diagram from combustion model ($\phi=0.5$, $\alpha=20$)

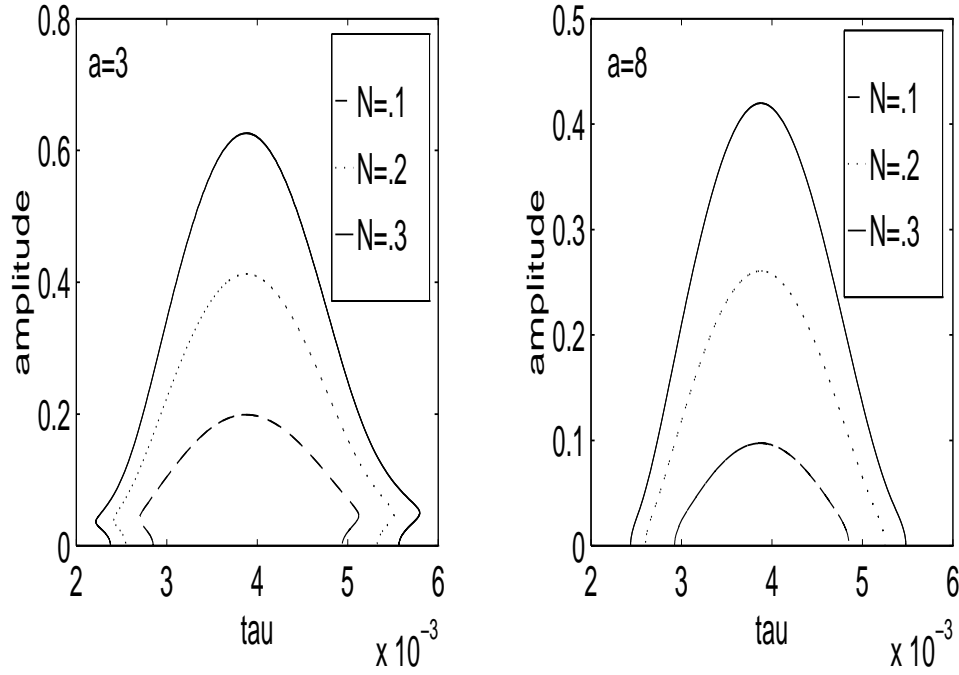


Figure 3: Variation of Amplitude with Delay

$\ddot{x} + x + x^2 = 0$). In the case of the combustion model considered in this paper, however, one may be able to use (26) with the same constant frequency, equal to the first instability frequency Ω and given by the linear analysis, for the reason that, in the whole operating range of parameters (20) can be treated as a perturbed linear system. Moreover, this frequency critically depends on natural frequency ω , damping α and delay τ but does not depend on other model parameters. This determines the domain of applicability of (26) with constant value of frequency Ω . Namely, fixing ω , α and τ , then compute the resonant frequency Ω from equation of (18) and varying, for example, gain N , it should be possible to predict the (averaged) behavior of the amplitude and its stationary values which will correspond to either stable or unstable limit cycles. Since (26) is a scalar equation, the stability of the stationary point (hence of the limit cycle) follows immediately: If r^* is a stationary point of (26), then it is stable when

$$\frac{N}{2\alpha\pi} \frac{d}{dr} \left[\int_0^{2\pi} H(\Omega r \cos(\varphi - \theta)) \sin \varphi d\varphi \right]_{r=r^*} < 1 \quad (27)$$

and unstable if the opposite inequality holds. Note that for small amplitudes this stability condition agrees with criticality computations outlined in the previous section.

In figure 3 limit cycle amplitudes as a function of delay is shown. This is computed using (26). The left and the right panels show diagrams for sub- and super-critical cases respectively.¹

¹In this computation we use nonlinearity in the form

$$H(u) = \begin{cases} S(\frac{a\bar{\phi}}{1+u}), & u \geq -1 \\ 1, & u < -1 \end{cases}; \quad S(x) = \frac{1}{1 + \exp(2 - x)}$$

The conclusions that are possible to derive from combustion model analysis to date are the following:

- The model shows limit cycling for a wide range of parameters.
- The stability boundary has a complicated structure, including interaction of different instabilities (for long delay τ).
- The third derivative of heat release nonlinearity is important for determining the type of criticality (supercritical vs. subcritical) for parameters on the stability boundary. It particularly affects our ability to generate cycling behavior with reasonably small amplitudes tracking only the nonsaturated part of the nonlinearity.
- The amplitude of oscillations is most sensitive to the delay parameter τ .

4 System Identification Methodology: A Case Study

The purpose of this section is to present the system identification methodology that has been applied to the combustion dynamics model. The methodology that is presented consists of identifying component subsystems using the available measurements and then checking that these component subsystems have the correct qualitative properties of a stable limit cycle and quantitative properties of amplitude and frequency of oscillation. The data used in this paper were obtained in an experimental program conducted by UTRC having the objective of demonstrating the applications of active control to lean premixed combustion systems [1]. The data consists of time records of pressure and heat release rate (global CH radiation intensity) for various power settings and equivalence ratios. The radiation intensity is assumed to be a measure of the rate of the heat release. A typical segment of the pressure and heat release data is shown in Figure 4.

One of the purposes of this section is to make comments on the selection of algorithms for the identification of component subsystems — these comments will necessarily be brief and further exposition is expected to be given in detail elsewhere. A different purpose of this section is to point out the need to be able to deal more effectively with identification of systems from limit cycle data, in particular, being able to enforce a priori the limit cycle behavior as opposed to the procedure presented that a posteriori checks the behavior.

A summary of some related work is as follows. The identification of linear systems from closed loop data (which is distinct from closed loop system identification from exogenous reference inputs) has been addressed in [13, 23, 22, 18] among others. Some of this work appears relevant to the case of nonlinear feedback and the details will be dealt with elsewhere. Some however is highly dependent on having linear feedback. The estimation of time delays can be found in multiple sources — see the references in [2]. The work on harmonic balance is taken from [8], see [15, 16] for a survey of related work that is applicable to check the qualitative properties of the system.

The remainder of this section is organized as follows. The identification of component subsystems as shown in Figure 1 are treated in separate sections; section 4.1 discusses the identification of linear acoustics, section 4.2 discusses the identification of the time delay, section 4.3 discusses the parameterization of the static nonlinearity and finally section 4.4 discusses the validation of the component subsystems relative to the final selection of gains and qualitative behavior of limit cycle dynamics.

with $\bar{\phi} = 0.5$.

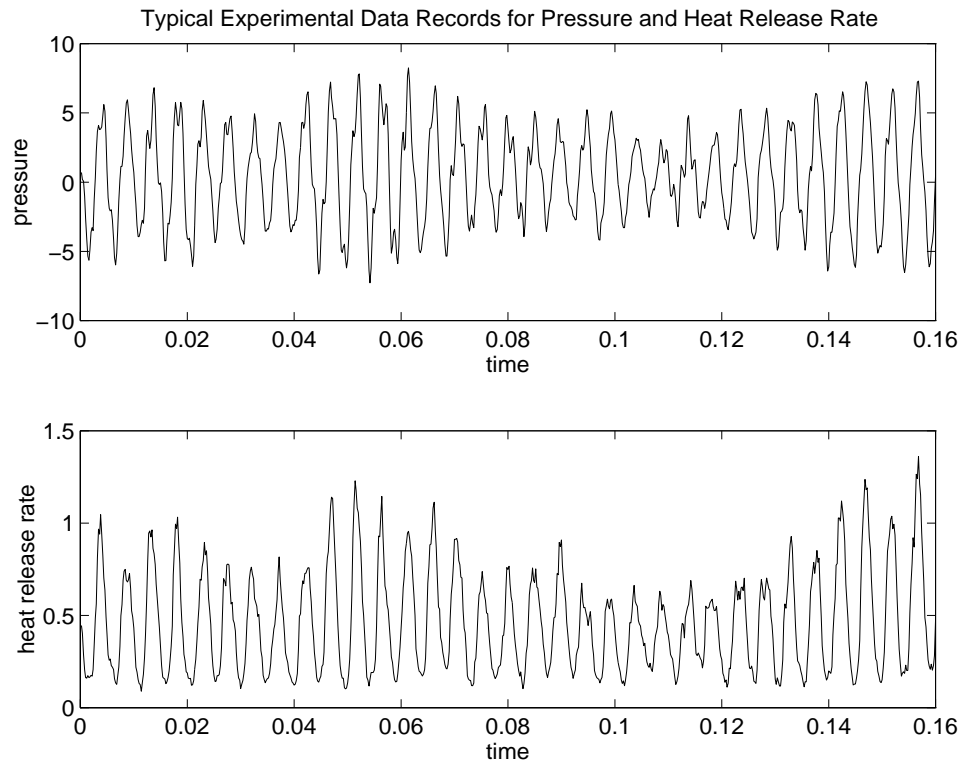


Figure 4: Time Records of Pressure and Heat Release Rate Obtained from UTRC/DARPA Single Nozzle Rig Experiment

Phi	ω_n (Hz)	ζ (%)
.56	(218,722)	(8.8,5.1)
.53	(239,741)	(13.4,4)
.51	(204,746)	(7.5,1.6)
.49	(197,739)	(6.9,.98)
.47	(192,737)	(8.4,2)

Table 1: Summary of Damping and Natural Frequencies for Identified Acoustics

4.1 Linear System Identification

The purpose of this section is to discuss the identification of linear acoustics as shown in the model structure in Figure 1. The problem is to utilize experimental measurements of heat release rate (q) and pressure (p) measurements to identify the acoustics labeled G in Figure 1.

The essential issue in this identification problem is that the measurements are taken in closed loop. That is, p, q are indeed measurements across the linear system G but there is feedback in the data. Moreover, in the model structure the feedback is nonlinear due to the nonlinear heat release function.

The issue with feedback in the data places constraints on the algorithms that may be used to recover the linear system. In particular in Figure 1 there are physical reasons for exogenous excitations at the output of G as well as the output of the nonlinearity H (the former because of fluid effects not caused by heat release forcing, such as vortex interactions, and the latter by heat release effects not caused by a velocity sensitive heat release, such as violations of the acuator disk model). The impact of these exogenous sources is that simple Fourier techniques (the empirical transfer function estimate) will not be reliable in estimating the linear system G ([22, 13].

The approach that has been adopted in the work to date is to use prediction error methods which are known to be consistent estimators in the presence of feedback provided that (a) correct noise models are chosen and (b) the feedback is linear [13, 23]. The extensions to the nonlinear feedback case considered here appear possible and will be dealt with elsewhere. The selection of a correct noise model is more problematic and future investigations will explore the use of nonparametric noise models as in the linear case [22, 21].

The data have been analyzed in the following manner. The heat release rate data has been differentiated to avoid identifying a known structural element. This new signal has been used as the input and the pressure data as the output. The results of using a Box-Jenkins parameterization is given in Figures 5 and 6 and Table 1 lists the results of applying the identification across of range of fuel-air ratios.

4.2 Time Delay Identification

The purpose of this section is to discuss the identification of the time delay in the model as shown in Figure 1. The time delay has been estimated in two ways and both methods give similar results. The first method is based on the nonparametric estimation of the nonlinearity as discussed more fully in section 4.3 and is limited mainly in the selection of the time delay to an integer number of time steps. This limits the resolution of the estimated time delay, moreover, any more subtle effects such as a time variation will not be captured by this method. The second method is based on a harmonic estimator and is able to overcome these two problems.

By finding an accurate estimate of time delay it may be possible to obtain a good nonparametric fit to the static nonlinearity H given by the model as shown in Figure 1. The model describes heat

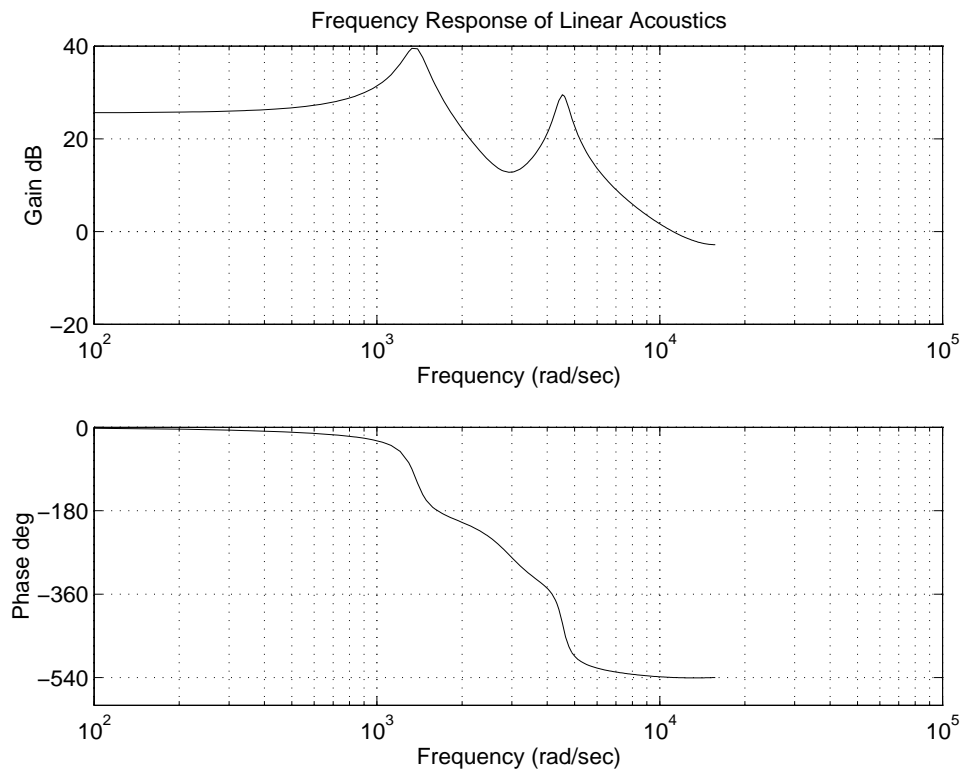


Figure 5: Frequency Response for R228 Pt42

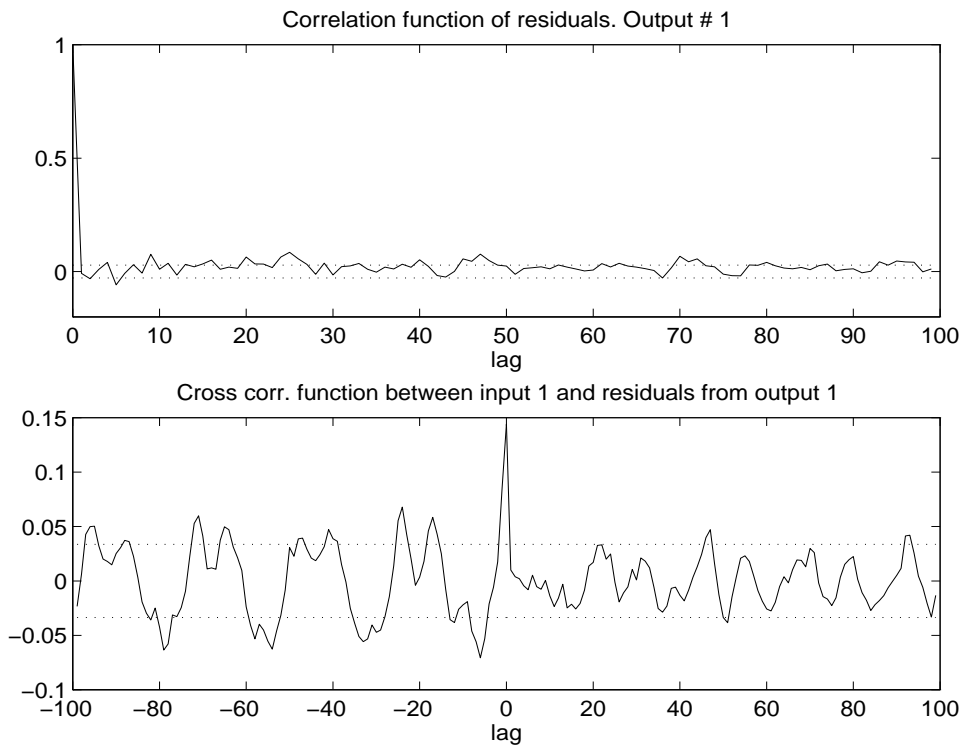


Figure 6: Residual Error Analysis for R228 Pt42

Equivalence ratio ϕ	Time delay $\hat{\tau}$ (sec)	Linear system frequency f (Hz)
0.56	0.00351	210
0.53	0.00356	209
0.51	0.00365	206
0.49	0.00381	202
0.47	0.00397	198
0.45	0.00472	177

Table 2: Bulk delay estimates for R228 data points.

release rate as a function of delayed velocity

$$q(t) = H(u(t - \tau)).$$

Thus if it were possible to plot $u(t - \tau)$ versus $\dot{q}(t)$ for various times t and a wide range of u 's, it would be possible to “trace out” the nonlinearity H (given that the model is accurate).

4.2.1 Bulk Delay Estimation

The data available for time delay estimation are measurements of pressure variations p' and heat release rate \dot{q} sampled at $f_s = 5000$ Hz at an operating fuel to air ratio ϕ . One delay estimation procedure consists of the following steps:

1. Remove DC bias from p' and low pass filter.
2. Noticing that p' can be well approximated by a sinusoid then it can be phase shifted by 90° by integration instead of differentiated to obtain a signal proportional to velocity.
3. Finally, a correlation between u and \dot{q} is performed to yield the bulk time delay estimate, i.e.

$$\hat{\tau} = \max_{\tau} E\{q(t)u(t - \tau)\}$$

Table 2 lists the estimated bulk delays for each data point obtained as a function of fuel-air ratio, ϕ , for the UTRC experiment.

4.2.2 Time-Varying Delay Estimation

The estimation in this section is based on the notion that pressure, velocity, and heat release rate data are close to periodic signals that can be approximated by sinusoids with the same frequency. Therefore, we use the approach from [2, p. 1498] which models signals u and \dot{q} as periodic signals perturbed by zero-mean white noise. Let z_k be one such discrete-time signal, described by

$$z_k = c + a \cos(\omega k) + b \sin(\omega k) + v_k$$

where v_k is zero-mean, white noise with variance R . This signal can be equivalently represented by the state-space system

$$\begin{aligned} x_{k+1} &= Fx_k \\ z_k &= H^t x_k + v_k \end{aligned}$$

with

$$\begin{aligned} F &= \begin{pmatrix} 1 & 0 & 0 \\ 0 & \cos(\omega) & \sin(\omega) \\ 0 & -\sin(\omega) & \cos(\omega) \end{pmatrix}, \\ H &= (1 \ 1 \ 0)^t \end{aligned}$$

and states

$$x_k = \begin{pmatrix} c \\ a \cos(\omega k) + b \sin(\omega k) \\ -a \sin(\omega k) + b \cos(\omega k) \end{pmatrix}.$$

A Kalman filter optimally estimates states x_k with observed states \hat{x}_k , minimizing

$$\mathbb{E}\{\|x_k - \hat{x}_k\|_2^2\}.$$

A time-invariant version of the Kalman filter — the steady state the harmonic component estimator — is given as

$$\begin{aligned} \hat{x}_{k+1/k} &= (F - KH^t)\hat{x}_{k/k-1} + Kz_k \\ \Phi_k^z &= C\hat{x}_k \end{aligned}$$

with $C = (0 \ 1 \ i)$, $K = FPH(H^tPH + R)^{-1}$ and $P = \epsilon I$, for some scalar $\epsilon > 0$ which controls the forgetting rate. Φ_k^z contains the phase information of z . The scalar ϵ serves as a gauge on the amount of state noise, or variations in frequency of the main harmonic. A very narrow bandpass filter uses small ϵ , has accurate steady-state performance (i.e. has less mean square state error norm) but has poor tracking abilities, while the opposite happens for large ϵ .

Hence, assuming u and \dot{q} are mostly sinusoidal, the time-varying delay estimate is given by the angle between Φ_k^u and Φ_k^q , i.e.

$$\hat{\tau}_k = \frac{1}{f_s} \frac{\text{sec}}{\text{sample}} \times \frac{1}{\omega} \angle \{\Phi_k^u (\Phi_k^q)^*\} \text{ sample}$$

The result of applying this time delay estimation is shown in Figure 7.

4.3 Parameterization of Static Nonlinearity

The purpose of this section is to discuss the parameterization of the static nonlinearity in the combustion model as shown in Figure 1. The parameterization is needed to produce a set of differential equations whose solutions may then be compared with the measured data.

The parameterization of the static nonlinearity proceeds from a nonparametric description — or graph — of the nonlinearity that follows directly once the time delay has been estimated as in section 4.2. The time delay estimate obtains a signal proportional to velocity by phase shifting the pressure signal by 90° , hence, once the time delay is known the same procedure allows variables across the nonlinearity to be obtained. These variables will be the input to the nonlinearity, $u(\cdot - \tau)$, and the output of the nonlinearity, $q(\cdot)$. These variables may then be plotted to obtain a nonparametric estimate of the nonlinearity.

The objective is to capture this nonparametric estimate of the static nonlinearity by a small number of parameters to complete a quantitative description by a small number of differential equations. The parameterization is not obvious due to the “scatter” on the nonparametric estimate.

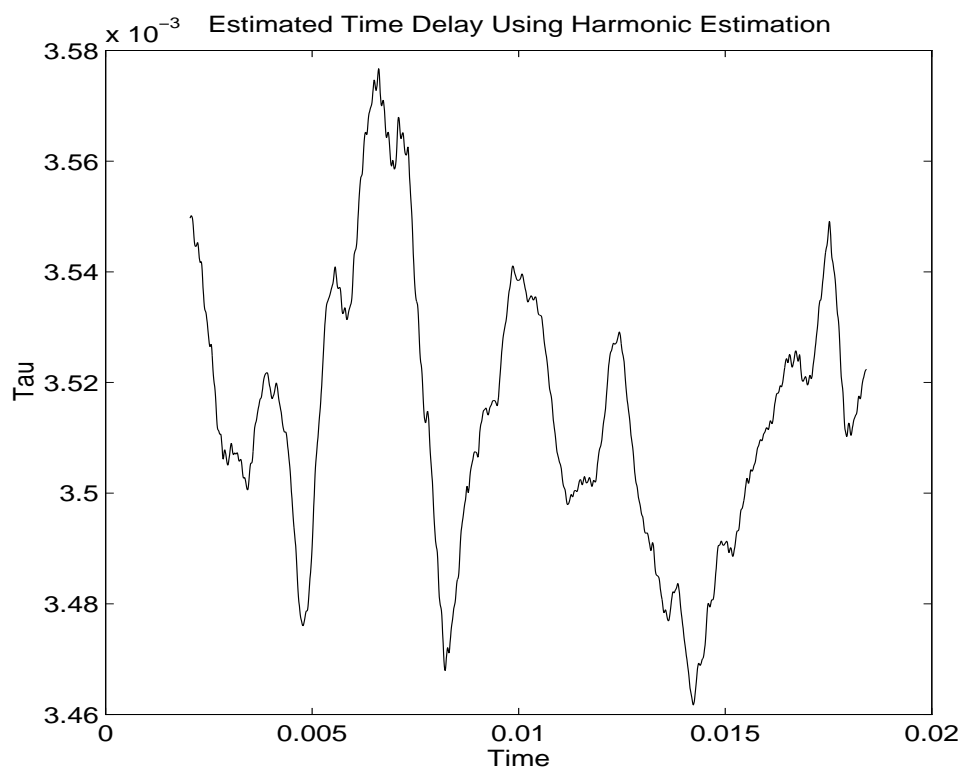


Figure 7: Time Delay Estimate R228 Pt42

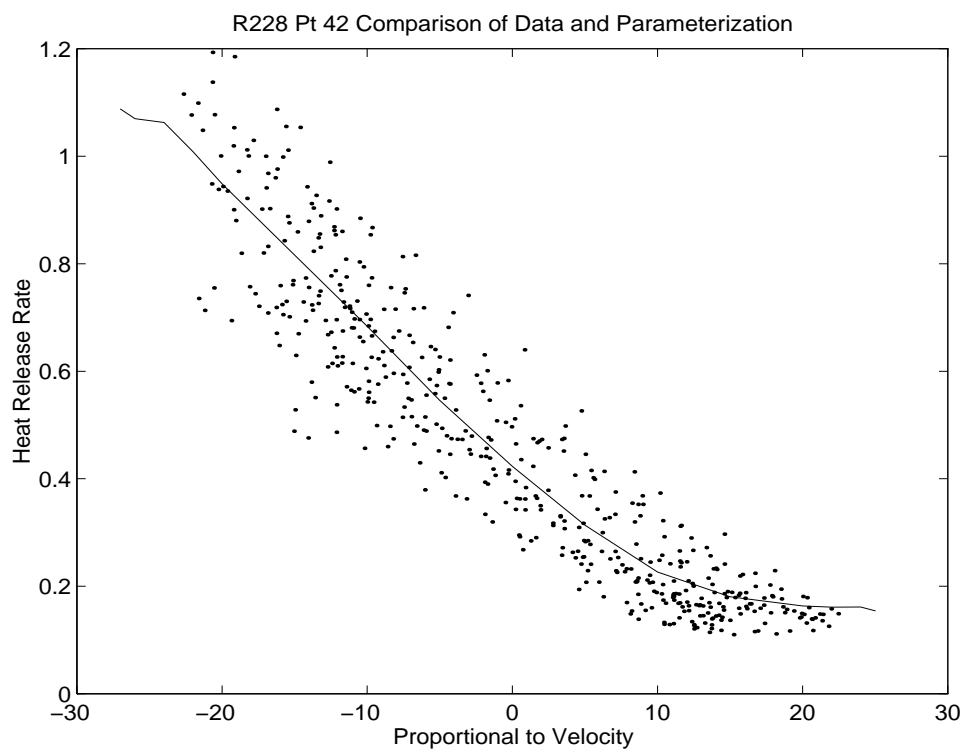


Figure 8: Parameterization of Nonlinearity R228 Pt42

A point of investigation is to resolve this “scatter” or at least to understand the source — further comments are made on this issue in section 5. In this section the “scatter” is effectively dealt with as if it were noise on the measurements.

One issue with obtaining a parameterization is to understand what the compression of the nonparametric estimate to a specific functional form influences. In addition it should be realized that a consistent approach should be taken to identify the static nonlinearity across different values of the fuel-air ratio.

The specific parameterization used in obtaining a final form of the static nonlinearity will influence — to a first order approximation — the amplitude of oscillation and the stability of the predicted limit cycle. These observations are a consequence of applying a first order (single sinusoid) harmonic balance technique as discussed in section 4.4. The current methodology is not to couple completely the parameterization to the harmonic balance, however, this could be done.

The method currently employed is to parameterize the nonlinearity by a piecewise linear function. The nonparametric representation by the graph is divided into bins on the velocity axis and the heat release rate values in these bins are averaged to obtain a single heat release rate value. The results of this method are shown in Figure 8.

4.4 Validation by Harmonic Balance

The purpose of this section is to describe the validation of the qualitative behavior of the entire dynamical system obtained from the component subsystems identified in the previous sections and shown in Figure 1. The problem is specifically to (a) take the identified linear system (G), time delay (τ) and parameterized nonlinearity (H) and determine if the combined system has a stable limit cycle and (b) select gains (N and scaling of the nonlinearity) so that the amplitude and frequency of the limit cycle matches that of the data (p, q).

The approach that has been adopted in this work to date is to validate qualitative behavior using harmonic balance methods. The use of harmonic balance allows the prediction of limit cycles, the stability of these limit cycles, and allows as well the selection of gains so that the amplitudes of observed limit cycles may be matched. Note that in the model structure adopted once the linear system and the time delay, hence overall system phase, of the system is chosen then, to a first harmonic approximation, the frequency of the limit cycle is determined and no more adjustment may be made.

The application of harmonic balance methods is illustrated in this paper for a single harmonic (usually called describing function analysis). Figure 9 shows the describing function for the parameterized nonlinearity in Figure 8. The harmonic balance equation for a single harmonic is

$$G(j\omega) = -\frac{1}{N(A)}$$

and the intersection of the Nyquist plot of G and the describing function is shown in Figure 10. The directionality of the intersection gives a heuristic for stability [8] (which may be sharpened as in [15]). The selection of gains to match amplitudes may be carried out on such a plot, specifically with reference to Figure 1 the amplitude of the velocity perturbations fixes the product $N\delta$ and then the knowledge of G and the heat release time series allows δ to be chosen and then hence N as well.

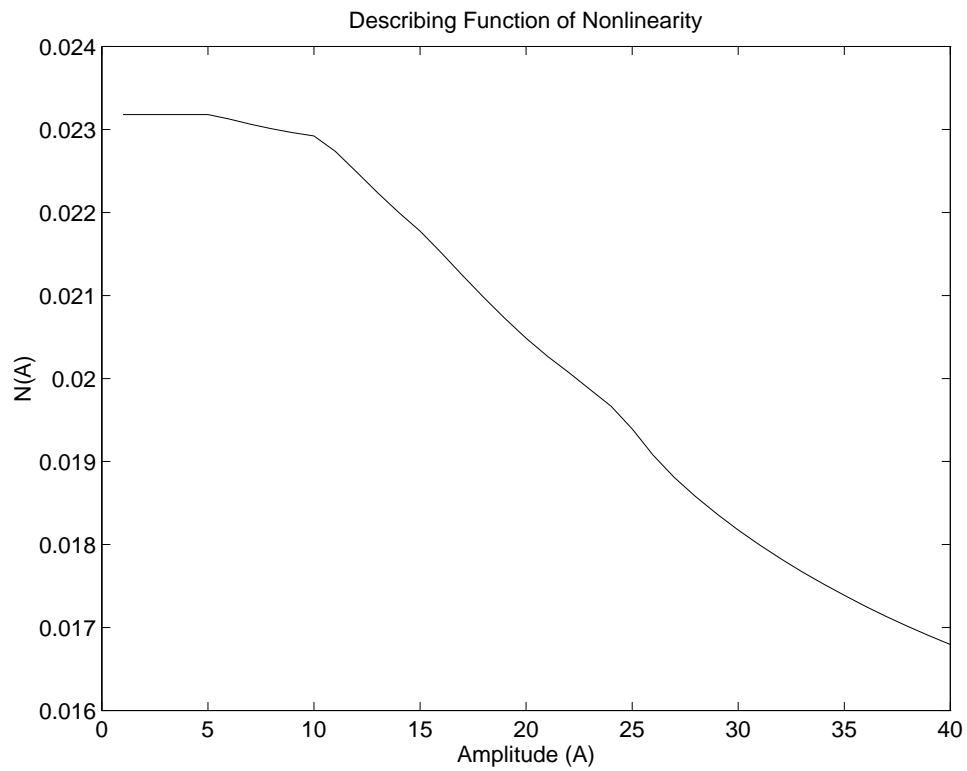


Figure 9: Describing Function of Parameterized Nonlinearity

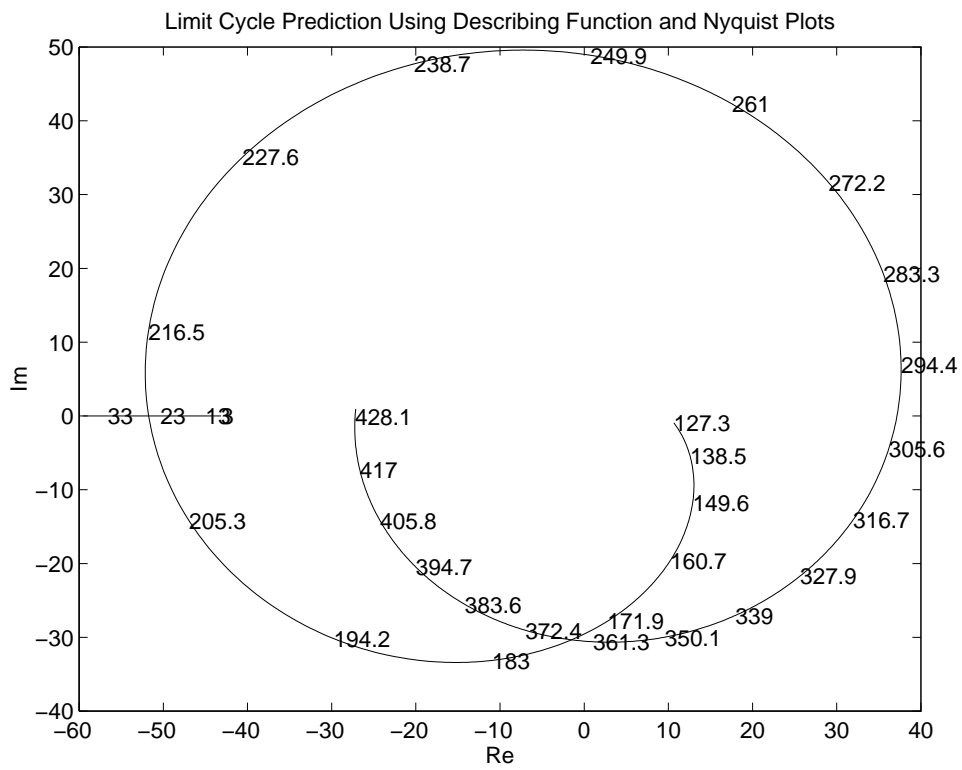


Figure 10: Describing Function Prediction of Amplitude and Frequency of Oscillation

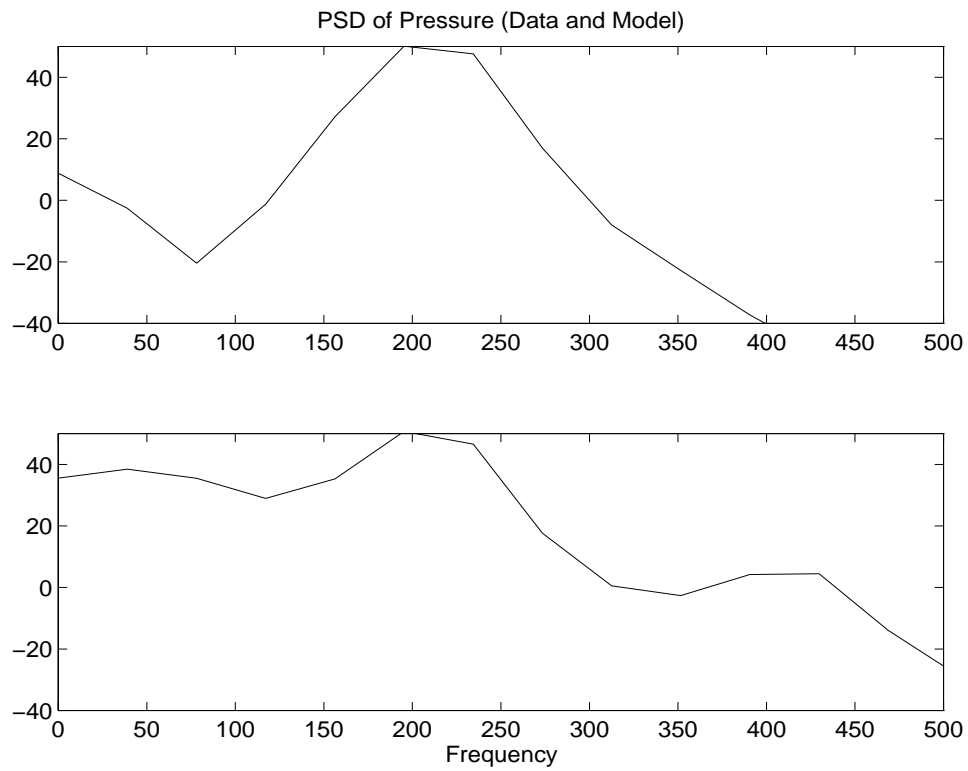


Figure 11: Comparison of Data and Model - Power Spectral Density of Pressure

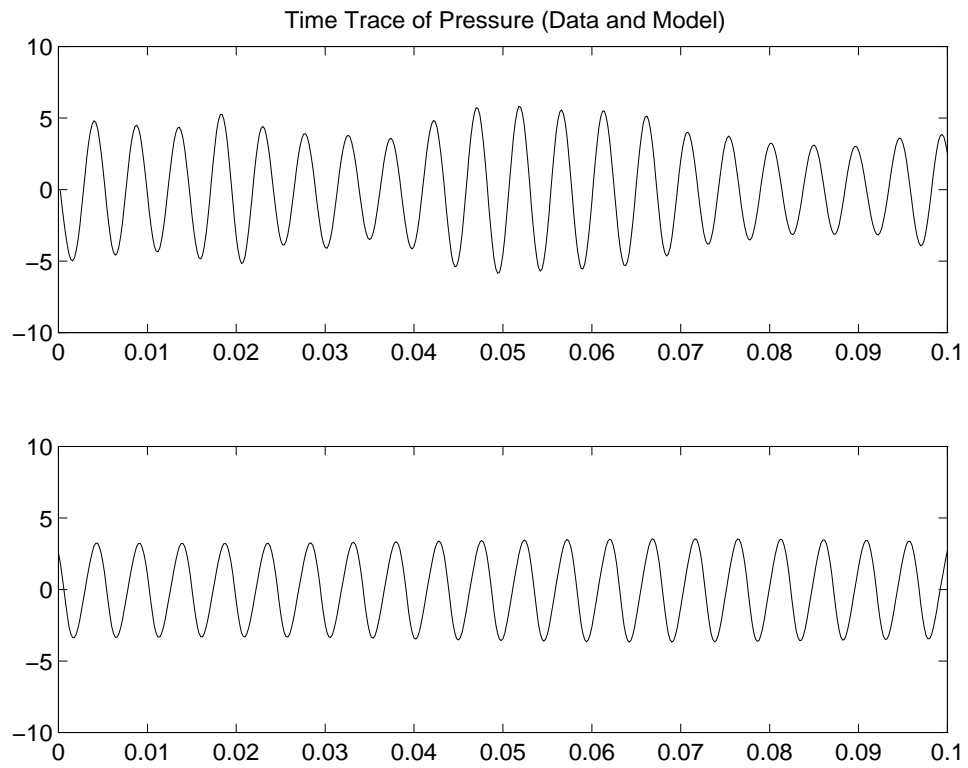


Figure 12: Comparison of Data and Model - Time Response of Pressure

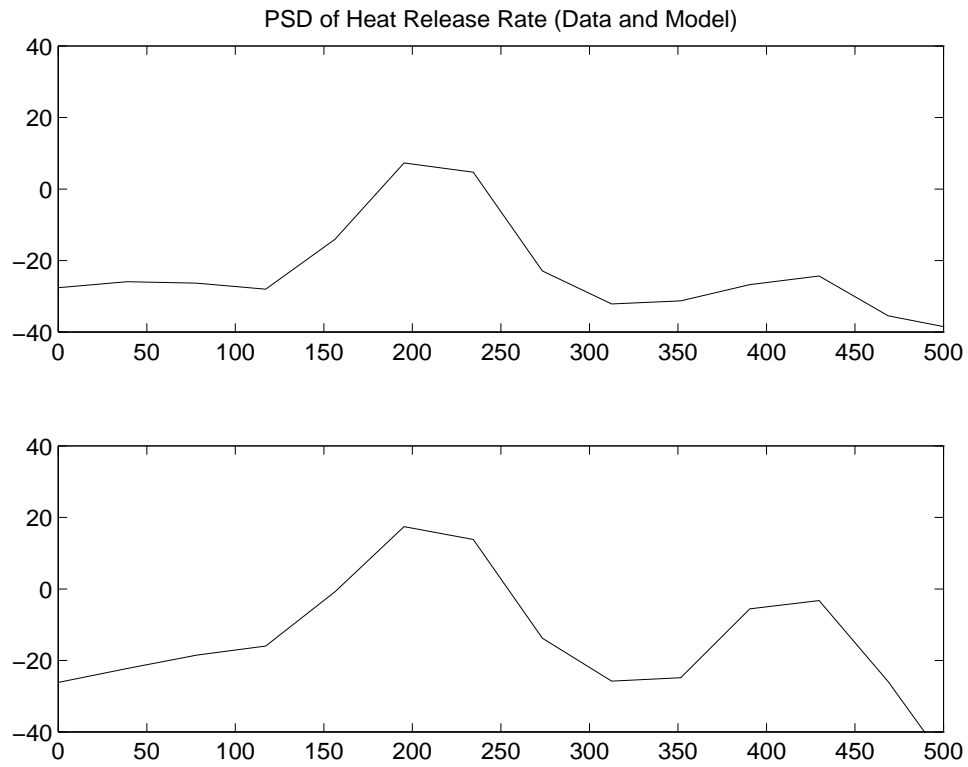


Figure 13: Comparison of Data and Model - Power Spectral Density of Heat Release Rate

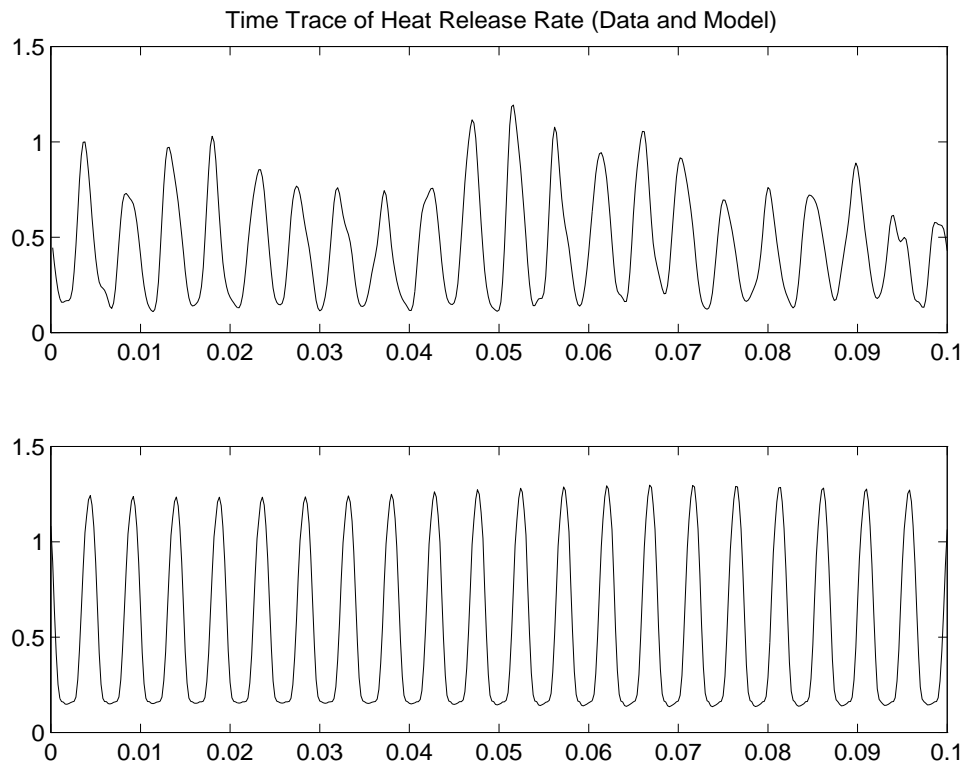


Figure 14: Comparison of Data and Model - Time Response of Heat Release Rate

5 Concluding Remarks

This paper has presented a study in system identification for limit cycling systems. An application that is of technological relevance has been presented to motivate the overall problem and application of standard estimation algorithms has been carried out on representative data.

This paper points to a need to develop theory and algorithms, in short, better understanding, of system identification techniques for limit cycling systems. Comments were made on the potential use of other standard methods, however, the authors are not aware of techniques that completely address issues in dealing with limit cycle data. In particular, it is not clear how to impose limit cycle dynamics onto the identification process. The paper has shown how to use standard analysis tools — which can be extended and sharpened beyond their use here — to confirm certain dynamical behavior of the final system, however, the apriori imposition of these behaviors on the overall identification procedure is not known.

6 Acknowledgments

The authors acknowledge support throughout the period of work reported in this paper from Drs. Rosfjord, McVey, Cohen and Rey of United Technologies Research Center.

References

- [1] Active control for marine and land based aeroderivative gas turbine engines, 1995. DARPA Contract MDA 972-95-C-009.
- [2] R.R. Bitmead, A.C. Tsoi, and P.J. Parker. A Kalman filtering approach to short-time fourier analysis. *IEEE Transactions on Acoustics, Speech and Signal Processing*, 34(6):1493-1501, December 1986.
- [3] S.M. Candel. Combustion instabilities coupled by pressure waves and their active control. *The Combustion Institute*, 1992.
- [4] F.E.C. Culick, W.H. Lin, C.C. Jahnke, and J.D. Sterling. Modeling for active control of combustion and thermally driven oscillations. In *Proceedings of the 1991 American Control Conference*, pages 2939-2948. IEEE, 1991.
- [5] A.P. Dowling. Nonlinear acoustically coupled combustion oscillations. In *2nd AIAA/CEAS Aeroacoustics Conference*. AIAA, 1996.
- [6] M. Fleifil, A. M. Annaswamy, Z. A. Ghoniem, and A. F. Ghoniem. Response of a laminar premixed flame to flow oscillations: A kinematic model and thermoacoustic instability results. *Combustion and Flame*, 106:487-510, 1996.
- [7] Y.-T. Fung and V. Yang. Active control of nonlinear pressure oscillations in combustion chambers. *J. Propulsion and Power*, 8(6):1282-1289, November-December 1992.
- [8] A. Gelb and W.E. Vander Velde. *Multiple-Input Describing Functions and Nonlinear System Design*. McGraw-Hill, New York, 1968.
- [9] J. Guckenheimer and P. Holmes. *Nonlinear Oscillations, Dynamical Systems and Bifurcations of Vector Fields*. Springer Verlag, New York, 1983.

- [10] J. K. Hale. *Theory of Functional Differential Equations*. Springer Verlag, New York, 1977.
- [11] B. Hassard, N. Kazarinoff, and Y.-H. Wan. *Theory and Application of the Hopf Bifurcation*. Cambridge University Press, 1981.
- [12] J.P. Hathout, A.M. Annaswamy, M. Fleifil, and A.F. Ghoniem. A model-based active control design for thermoacoustic instability. Technical Report 9703, MIT, 1997.
- [13] L. Ljung. *System Identification*. Prentice-Hall, Englewood Cliffs, NJ, 1987.
- [14] K.R. McManus, T. Poinso, and S.M. Candel. A review of active control of combustion instabilities. *Prog. Energy Combust. Science*, 19:1–29, 1993.
- [15] A. I. Mees. *Dynamics of Feedback Systems*. Wiley, New York, 1981.
- [16] A.I. Mees. Describing functions: Ten years on. *IMA J. Applied Mathematics*, 32:221–233, 1984.
- [17] A.A. Peracchio and W. Proscia. Nonlinear heat release/acoustic model for thermoacoustic instability in lean premixed combustors. In *1998 ASME Gas Turbine and Aerospace Congress*. ASME, 1998.
- [18] R. Pintelon, P. Guillaume, Y. Rolain, and F. Verbeyst. Identification of linear systems captured in a feedback loop. *IEEE Transactions on Instrumentation and Measurement*, 41(6):747–754, December 1992.
- [19] S.A.Campbell. Resonant codimension two bifurcation in a neutral functional differential equation. In *Proceedings of the 1996 World Congress of Nonlinear Analysts*, 1996.
- [20] J. Sanders and F. Verhulst. *Averaging Methods in Nonlinear Dynamical Systems*. Springer Verlag, 1985.
- [21] J. Schoukens and R. Pintelon. *Identification of Linear Systems*. Pergamon Press, Oxford, 1991.
- [22] J. Schoukens, R. Pintelon, G. Vandersteen, and P. Guillaume. Frequency domain system identification using nonparametric noise models estimated from a small number of data sets. *Automatica*, 33(6):1073–1086, 1997.
- [23] T. Söderström and P. Stoica. *System Identification*. Prentice-Hall, Englewood Cliffs, NJ, 1989.
- [24] B.T. Zinn and Y. Neumeier. An overview of active control of combustion instabilities. In *35th Aerospace Sciences Meeting*, 1997.